PERIODICA POLYTECHNICA SER. TRANSP. ENG. VOL. 23, NO. 1-2, PP. 89-105 (1995)

COMPUTER SIMULATION STUDY OF THE INFLUENCE OF TOOTH ERRORS ON GEAR DYNAMIC BEHAVIOUR

János MÁRIALIGETI

Department of Machine Elements
Technical University of Budapest
H-1521, Hungary

Received: November 1, 1994

Abstract

The origin of the excitation effects of gear train is briefly discussed and an adequate tooth spring system model is presented, which enables to take into consideration the important exiting effects, due from the mesh. The model is especially adapted for computer simulation studies. Making use of this tooth mesh substituting model, the basic tooth vibration features are discussed, based on simulation results. Influence of the mesh irregularities, being always present, even in the case of ideal toothing, is presented. Further on, the effect of the manufacturing errors on gear dynamic behaviour is analyzed by the Furier development of the tooth stiffness functions on one hand, and the vibration characteristics are studied under quasi stationary rolling down conditions, based on computer simulation results, on the other hand.

Keywords: gear dynamic, computer simulation, non-linear vibration, parametric excitation, tooth errors.

1. Introduction

The gear transmissions are one of the mostly applied power transmission elements in mechanical drive systems. In the case of their application in vehicle transmissions, they are generally subjected to random load conditions, varying in a wide range of load levels and excitation frequencies. The schematic model of a drive system is represented on *Fig. 1*. The gear box on the input is connected to the prime mover, providing a variable $T_1(t)$ input torque and on the output it is coupled to the final drive, presenting a variable $T_2(t)$ load as well, where t is the time. Both are varying in the load and in the frequency range, too.

The gear trains as active vibration exciting elements can have important effect on the dynamic behaviour of the whole transmission system. They influence the load histories on the connected parts on one side and their own load conditions on the other side. On *Fig. 1* $s(\varphi_1)$ refers to the vibration exciting effect, as a function of the input φ_1 angular displacement.

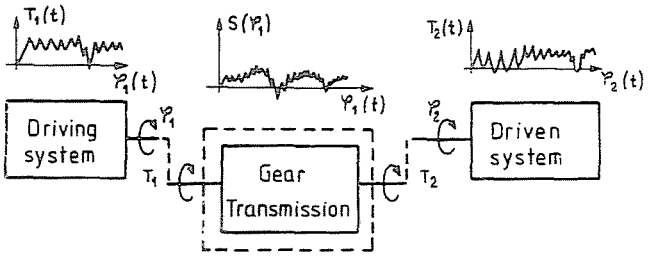

Fig. 1. Schematic representation of a vehicle drive system

Because of the complexity of the problem, numerical simulation technics can be applied for system and for element characteristic analysis and optimisation [1, 2].

In this contribution, some basic aspects of the non-linear vibrations of gear trains are studied and some simulation results are presented for gears with ideal normal and modified involute profiles and for gears with manufacturing errors, as base circle and pitch error.

2. The Origin of the Vibration Exciting Effects of Gears

The main vibration exciting effects of gears can be originated by two main groups [3,4]:

- The effects caused by the stiffness variation of the teeth, on two levels, namely the stiffness variation as the function of the contact point location of the mating single tooth pairs and the alternating number of teeth being actually in mesh. They are called generally as dynamic effects.
- The effects introduced by contact irregularities at the beginning and at the end of the pressure line, even in the case of ideal geometry, and the exciting effects introduced by manufacturing errors and intended profile modifications, the latter for improving gear characteristics. They are called generally as cinematic excitation effects.

Other parameters as the friction influence are generally less important.

In the case of ideal tooth meshing, assuming that the teeth under load do not deform, the stiffness variation can be described in the function of the drive gear angular displacement, φ_1, as a simple periodic function, $s(\varphi_1)$, where the period is determined by the angular displacement corresponding to a single tooth contact length, $\Omega_z = \gamma_{1b}$. At that model, the abrupt stiffness change is accepted at the end points φ_{A_i} and φ_{E_i} of the pressure line, see *Fig. 2a*. The load influence on the meshing characteristics is fully neglected, so the resulting vibration is linear: no load influence is present.

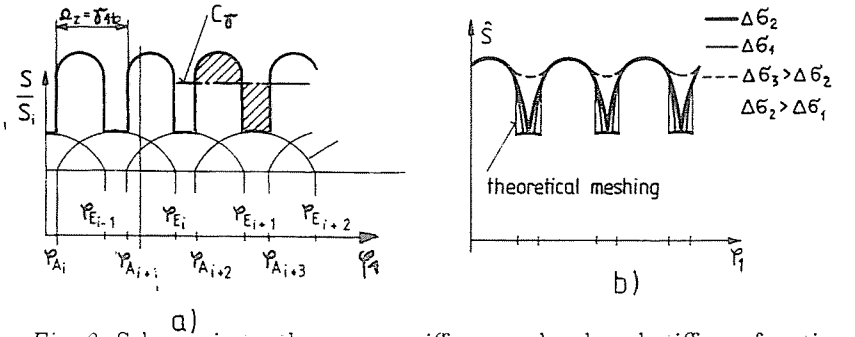

Fig. 2. Schematic tooth contact stiffness and reduced stiffness functions

However, even in the case of ideal tooth geometry, assuming elastic tooth deformations under load, the tooth contact length varies in the function of the load, so the stiffness function must be replaced by a two variable function, $\hat{s}(\varphi_1; F_N/b)$, where F_N/b is the specific tooth normal load, F_N stands for the tooth normal force, and b is the tooth length. The $\hat{s}$ *reduced stiffness function* [4] contains already the load influence, so the resulting vibration will not be linear. On the *Fig. 2b*, the load dependent stiffness variation is schematically represented for *ideal geometry and realistic tooth meshing*, i.e. the tooth deformations are taken into consideration. $\Delta\sigma$ refers to the specific load as parameter. If real tooth with fabrication error is considered, the period of the $\hat{s}(\varphi_1; F_N/b)$ function is determined by the angular displacement of the drive gear, corresponding to the all possible combinations of contact of the drive and of the driven gear tooth profiles.

The tooth fabrication errors, as pitch, profile, etc. errors, result in the non-uniform rotation transmission, see for ex. *Fig. 3* for the profile error, resulting non-linear effects, too. The influence of the intended profile modification is load dependent as well.

Further non-linear feature is introduced by the non-linear single tooth pair force-deflection characteristic at any fixed contact point, resulting variable stiffness in the function of the load, see for ex. [5]. On the *Fig. 4*, single tooth pair force-deflection curve is schematically represented, where w stands for the tooth deflection. The theoretical, linear force-deflection curve is indicated as a thin line.

The linear vibration model, discussed in detail by many authors, is convenient for qualitative studies, or in the case of constant load drives, if the specific load is in the middle or high load range. In vehicle drive systems, however, characterised by important load variations, the load dependent effects must be taken into consideration, so the non-linear gear vibration properties are of prime importance.

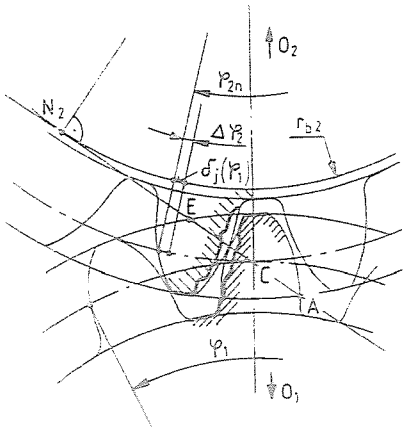

Fig. 3. Real tooth profile meshing (schematic)

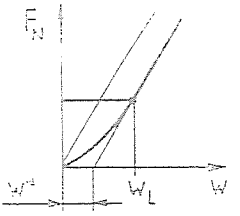

Fig. 4. Non-linear single tooth pair force-deflection curve

3. Gear Train Modelling and Basic Tooth Dynamic Behaviour

3.1. The Gear Train Model

For the study of the gear dynamic behaviour, a two mass model is applied, see *Fig. 5a*, where the two rotating masses are coupled by a system of springs, replacing the real tooth mesh, see *Fig. 5b*, where T_1, T_2 are the torques, r_{b1}, r_{b2} are the base circle radii, φ_1, φ_2 are the real angular positions, z_1, z_2 are the number of teeth, J_1, J_2 are the moments of inertia, i_n is the *nominal ratio*, $\bar{s}_j(\varphi_1)$ is the single tooth pair stiffness, K_j is the damping coefficient, b is the backlash. *Contact function* $\delta_j(\varphi_1)$ [4], corresponds to the j-th tooth profile pair combination, and gives the travel along the pressure line, corresponding to angular error $\Delta\varphi_2 = \varphi_{2n} - \varphi_2$ of the driven gear, in the case of zero load, only the j-th tooth pair being in contact, where $\varphi_{2n} = \varphi_1 / i_n$ is the nominal angular position. F_z and F_D are the elastic and the damping force components of the tooth normal force. The values with mark correspond to the reverse torque transmission.

The model enables the handling of the reverse torque transmission case, and the individual treatment of the different tooth pair characteristics, so single

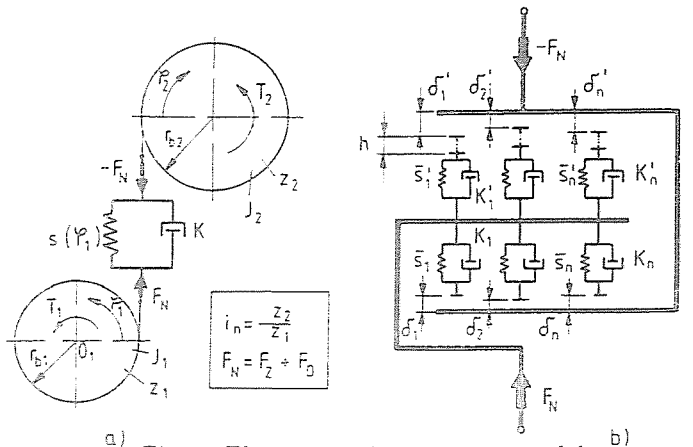

Fig. 5. The gear train two mass model

tooth error influences can be modelled as well.

The equation, corresponding to the system takes the following form:

$$J_1\ddot{\varphi}_1 + \left[\sum_{j=1}^{n} K_j \cdot \left(\Delta\dot{\sigma} - \dot{\delta}_j(\varphi_1)\right)\right] \cdot r_{b1} + \quad r_{b1} \cdot \hat{s}(\varphi_1 : \Delta\sigma) \cdot \Delta\sigma = T_1(t),$$

$$J_2\ddot{\varphi}_2 + \left[\sum_{j=1}^{n} K_j \cdot \left(\Delta\dot{\sigma} - \dot{\delta}_j(\varphi_1)\right)\right] \cdot r_{b2} + \quad r_{b2} \cdot \hat{s}(\varphi_1 : \Delta\sigma) \cdot \Delta\sigma = -T_2(t) \quad (1)$$

where the points stand for the time derivatives, $\Delta\sigma = r_{b1} \cdot \varphi_1 - r_{b2} \cdot \varphi_2$ is the travel error of the wheel measured on the pressure line, corresponding to the actual angular position, relative to the nominal angular position, so the term $\hat{s}(\varphi_1 : \Delta\sigma) \cdot \Delta\sigma$ gives directly the actual elastic total force in the tooth contact.

The $\hat{s}(\varphi_1 : \Delta\sigma)$ reduced stiffness function contains all vibration exciting effects, and formally can be applied as multiplication factor with the actual deformation. In the general form, it can be developed by its Fourier components:

$$\hat{s}(\varphi_1 : \Delta\sigma) = C_0(\Delta\sigma) + \sum_{k=1}^{\infty} C_k(\Delta\sigma) \cdot \cos\left(\frac{2\pi}{\Omega} \cdot k\varphi_1 + \nu_k\right) \quad (2)$$

where the load dependence is symbolised by the actual 'deflection' value $\Delta\sigma$ C_0 is the load dependent average, C_k is the k-th Fourier component, Ω is the basic period, and ν_k stands for the phase angle.

As it is known, this vibration exciting type belongs to the group of the *rheo-non-linear* vibrations [6]. Because of the composed parametric excitation function, *Eq.* (2), analytic solutions are not possible. The convenient way for the study of the dynamic behaviour is the computer simulation.

Further on, the basic vibration properties of a simplified system will be presented.

3.2. Basic Dynamic Behaviour.

The basic vibration properties of a simple one mass system with harmonic excitation can be studied by the *stability chart*, see ex. [6].

Introducing into the *Eq.* (2) an $\Omega = 2\pi$ periodic excitation function with $k = 1, \nu_k = 0$ and assuming a load independent case, we get a simple cosine type excitation, see *Fig. 6*, where $\tau = \omega_1 \cdot t$ is a dimensionless parameter, ω_1 being the input angular speed. Reducing the system of *Eq.* (2) into a one mass system [7], the resulting homogeneous differential equation is a rheo-linear, Matthieu type one.

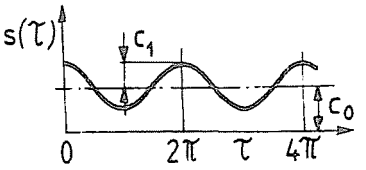

Fig. 6. Simple cosine type excitation function

The ω_s system eigenfrequency in this case is $\omega_s = \sqrt{C_0/m}$, where $C_0 = c_y$ is the *gear engagement spring stiffness* [8], and m is the reduced mass of the one mass system. The tooth angular frequency $\omega_z = \omega_1 \cdot z_1 = 2\pi f_z$, where f_z is the tooth frequency. It can be concluded from the stability chart, that at ω_1 input speeds of:

$$\omega_1 = \frac{2 \cdot \omega_s}{v}; \quad v = 1, 2, \ldots, \infty \tag{3}$$

resonance points develop. In the gearing technics, the resonance point corresponding to $v = 2$ is called as main resonance. Introducing the N dimensionless number by:

$$N = \frac{\omega_1 \cdot z_1}{\omega_s} = \frac{2}{v} \tag{4}$$

the resonance points are at $N = 2, 1, (2/3), 1/2, (2/5)\ldots$, and the main resonance corresponds to the value of $N = 1$. The N values in parenthesis,

corresponding to the odd values of v, are generally not important, and do not develop in the presence of damping.

The *excitation intensity* can be characterised by the $C_k' = C_k/C_0$ *excitation intensity factor*. Greater intensities give broader resonance regions, characterised by more intensive vibrations, even in the case of the presence of damping and inversely.

For the simulation study of gear vibration, one can generate by computer simulation quasi stationary resonance curves, by simulating an acceleration process at a given nominal static specific tooth normal load, from n_1 zero speed over the main resonance point. The diagram ordinate on the resonance curves is the dimensionless V_Σ value, the *contact force magnification factor*, defined by the following equation:

$$V_\Sigma = \max_{\gamma_{1b}} \{V_\Sigma(\varphi_1)\} \; ; \qquad V_\Sigma(\varphi_1) = \frac{\sum_{j=1}^{n} \frac{F_{Nj}(\varphi_1)}{b}}{\frac{F_N}{b}} \tag{5}$$

where F_N/b is the total constant specific load on the teeth, and F_{Nj}/b is the real dynamic specific tooth load on the individual tooth in mesh, n is the number of teeth actually in mesh, γ_{1b} is the rotation angle on the drive gear, corresponding to one tooth mesh.

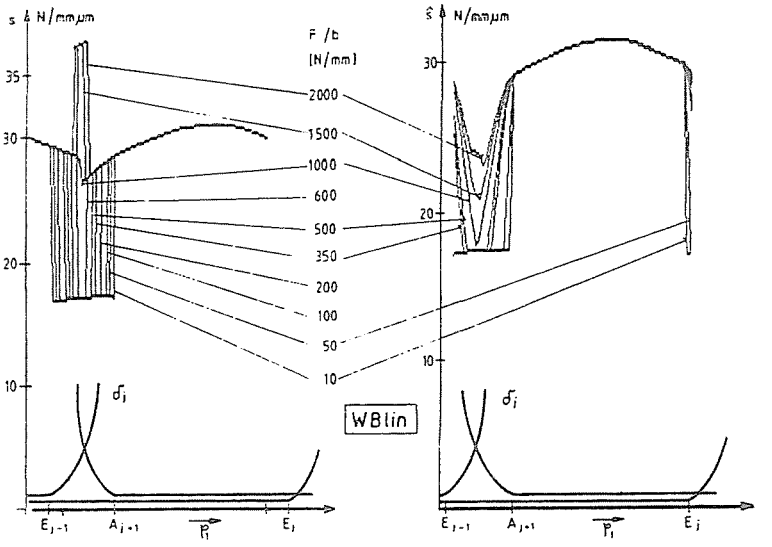

Fig. 7. Stiffness functions for an ideal gear train, with real meshing

For real gear vibration excitation functions, *Eq.* (2), generally the $k \neq 1$, nevertheless the basic characteristics of the parametric vibrations can be fairly well represented with an ideal gear train model.

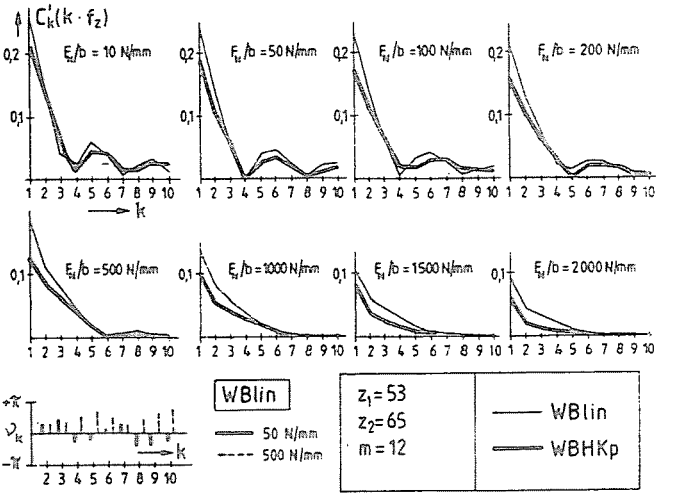

Fig. 8. Vibration exciting intensity components for ideal gear with real meshing

To demonstrate the basic behaviour of a rheo-linear system as a reference one, an ideal gear train model behaviour is simulated, with a quasi stationary acceleration process. A linear single tooth pair force-deflection characteristic, so constant stiffness at each contact point is applied. Evidently, the stiffness values vary from point to point. Further on, the code WBlin refers to this type of stiffness characteristic. The tooth deformations, so the load dependent pressure line length is taken into the calculation, see *Fig. 2b*. Consequently, the system is not exactly linear, but at a constant specific load, it can be accepted as a good approximation.

Fig. 7 represents the $\hat{s}\ (\varphi_1; F_N/b)$ reduced stiffness function, which is the excitation one, and the $s\ (\varphi_1; F_N/b)$ function, which represents the stiffness variation. The latter determines the system eigenfrequency. The nominal (at zero load) contact ratio for this train is $\varepsilon_\alpha = 1{,}7$, so at high specific load values the $\varepsilon_\alpha > 2$. The δ_j *contact functions* for the individual teeth enable to follow the mesh conditions of the gears [4]. *Fig. 8* shows the reduced Fourier components of the excitation function, the C'_k excitation intensity factors. The code WBlin refers to a linear single tooth stiffness characteristic.

Fig. 9a represents the resonance curve for this gear variant. For the simulation, the $h = 0$ backlash value was chosen, for avoiding the non-linearities involved in the case of tooth flank separations. A fairly low, $D_z = 0.007$ Lehr damping ratio was chosen, to assure the development of the resonance points.

The gear and other parameters are given on the Figure. The marked N values show the resonance locations. At lower speeds, even in the case of a small damping, the resonances cannot develop. The relatively small

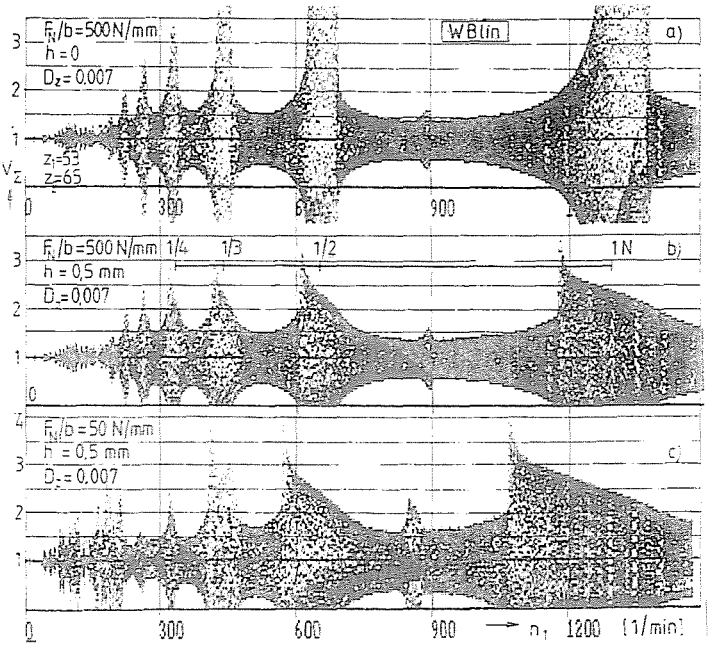

Fig. 9. Resonance curves for ideal gear, real meshing, with low damping ratio

elevations at $n_1 = 900/\text{min}$ refer to the resonance at $N = 2/3$. The Figure shows that at lower speeds the vibrations are relatively reduced, but at the value of about 200/min, important vibrations are present. Especially the resonances at $N = 1, 1/2, 1/3, 1/4$...are important.

Further on, several parameters, introducing non-linearity, are studied.

4. Non-linear Vibrations in the Case of Ideal Gear Geometry

For the study of the effects of some basic gear parameters and meshing properties introducing non-linearity, the previously applied real gear train with ideal geometry was chosen. Real tooth engagement was applied in all cases.

The real tooth engagement means that the pressure line length is load dependent, so the reduced stiffness function, so the excitation properties vary in the function of the load. Further on, the variable contact length influences the average damping as well. So, the influence of the nominal load, the realistic backlash and the non-linear single tooth characteristic was studied. For all cases, quasi stationary acceleration or deceleration processes were simulated and the ratio of the contact force magnification factor was calculated, see *Eq.* (5).

Fig. 9b represent the basic effect of the backlash, involving important

non-linearity. For the sake of the better representation of the basic features, the previously applied damping ratio was applied. The $V_{\underline{x}} = 0$ values indicate the separation of the tooth flanks, enabled by the presence of the backlash. Characteristic non-linear resonance shapes develop, with reduced peak values, as compared to the case of *Fig. 9a*. Because of the average stiffness reducing effect of the backlash, the resonance regions are at lower speeds. *Fig. 9c* represents the influence of the nominal specific load, in accordance with the reduced stiffness exciting components on *Fig. 8*. The increase of the vibrations at the resonance points involves increased tooth flank separations, so the resonance locations move to the direction of lower speeds. Because of the increased C'_k values, the vibrations are more intensive, with increased contact force elevation factors.

Fig. 10 presents the simulation results for the same gear train, with backlash and realistic damping ratio, in the case of WBlin, linear single tooth pair stiffness characteristic. At lower nominal specific load values the tooth flank separation remains at the resonance points, however, at higher specific loads it disappears. The peak values are generally lower as in the cases of small damping, and the higher order resonances tend to disappear. At F_N/b=1000 N/mm specific nominal load, the contact force magnification factors are considerably reduced, as it follows from the vibration exciting intensity factors.

The *Fig. 10b* shows a deceleration process. The opposite running direction of the main resonance point results in the broadening of the resonance region, and it extends to the resonance at N=1/2. This feature is well known in the field of the non-linear vibrations.

On *Fig. 12* the influence of the non-linear single tooth pair stiffness characteristic is presented. The applied stiffness curve type is as it is on the *Fig. 4*, with a progressive beginning section, and linear later. The stiffness reducing effect of the gear body design (as gear rim) was taken into account too [8]. The code for this single tooth pair stiffness characteristic is WBHKp. The reduced stiffness and stiffness function show important changes, related to the WBlin case, see *Fig. 11*. The Fourier components of the vibration exciting intensity are shown on *Fig. 8*.

Based on the resonance curves on *Fig. 12*, one can see that the vibration effects are smoother than for the WBlin case, see *Fig. 10*. The origin of it is the smooth beginning part of the single tooth pair stiffness curve, the smaller average stiffness and the increased contact ratio, resulting higher average damping. The load influence, however, is expressed.

At F_n/b=50 N/mm specific load, no tooth flank separation occurs, and the main resonance points are at lower speed, because at that load, the small stiffness region of the characteristic curve dominates. The resonances are reduced, too, related to the WBlin case. At high specific load values the contact force magnification factors decrease.

Based on the results of the simulations, one can state that even in the case of ideal tooth geometry, important non-linear behaviour is found. Con-

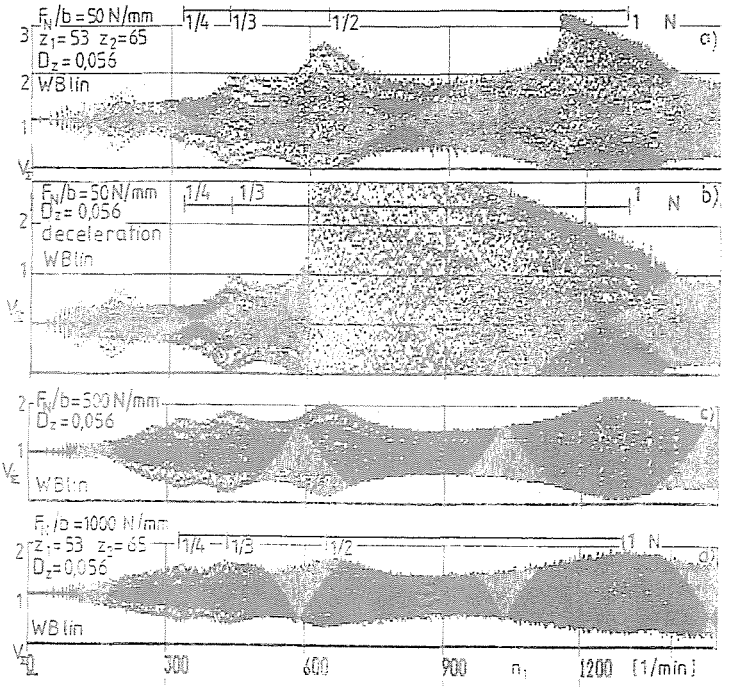

Fig. 10. Resonance curves for gear train with ideal geometry, real meshing and normal damping

sequently, in gear applications, characterised by important load variations, the non-linear effects can not be neglected.

5. Dynamic Behaviour in the Case of Gears with Profile Error

For the study of the profile error influence, the same gear train was applied. The profile error was taken onto the drive gear, as a base circle error on each tooth, of $f_{h\alpha} = -20$ μm, which corresponds to a DIN7 (ISO) quality class [9]. This driver was rolled together with the driven gear, having ideal tooth geometry.

On *Fig. 13* the reduced stiffness and the stiffness functions with the C'_k components, and the contact functions are shown, for linear single tooth stiffness characteristic (WBlin). The $\hat{s}$ excitation function changes considerably, related to the ideal geometry, especially at lower specific load levels. The C'_k excitation intensity factors increase similarly, especially at low specific load levels.

On *Fig. 14a* an h=0 backlash value was applied, for the sake of com-

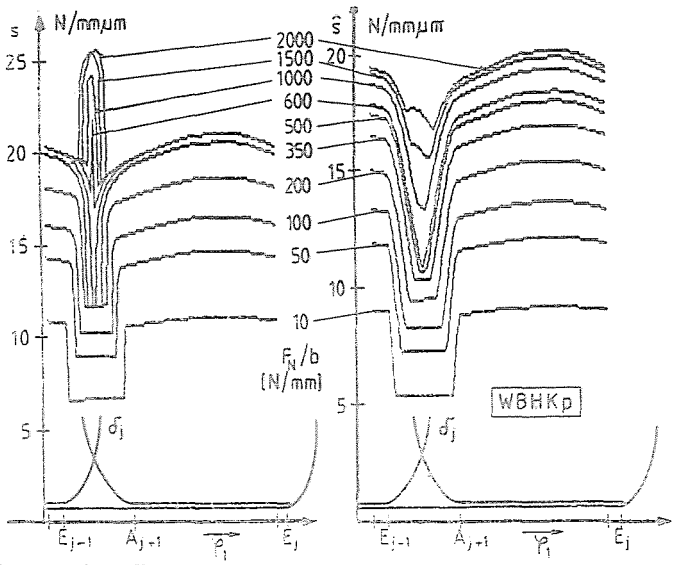

Fig. 11. Reduced stiffness and stiffness function for non-linear single tooth pair stiffness characteristic

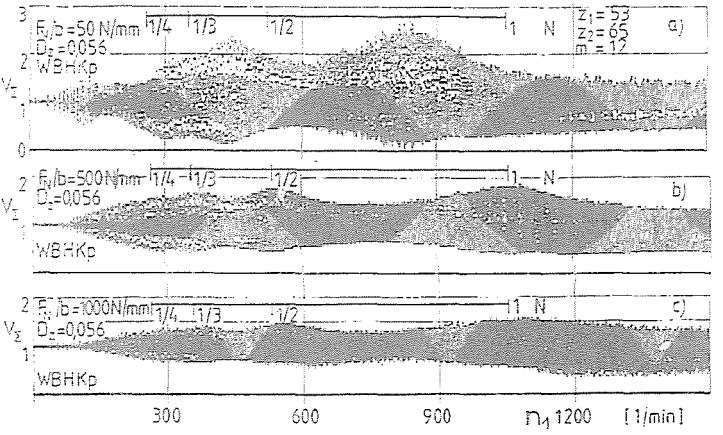

Fig. 12. Resonance curves for non-linear single tooth force-deflection characteristic

parison of the results on *Fig. 7a*. In spite of the normal damping, important vibrations develop, with an expressed hardening type non-linear resonance at the main resonance point. The *Fig. 14b* represents the resonance curve at the same specific load level as previously, with backlash. Because of the important vibration effects, tooth flank separations occur practically on the hole speed region, with important softening type non-linear resonances.

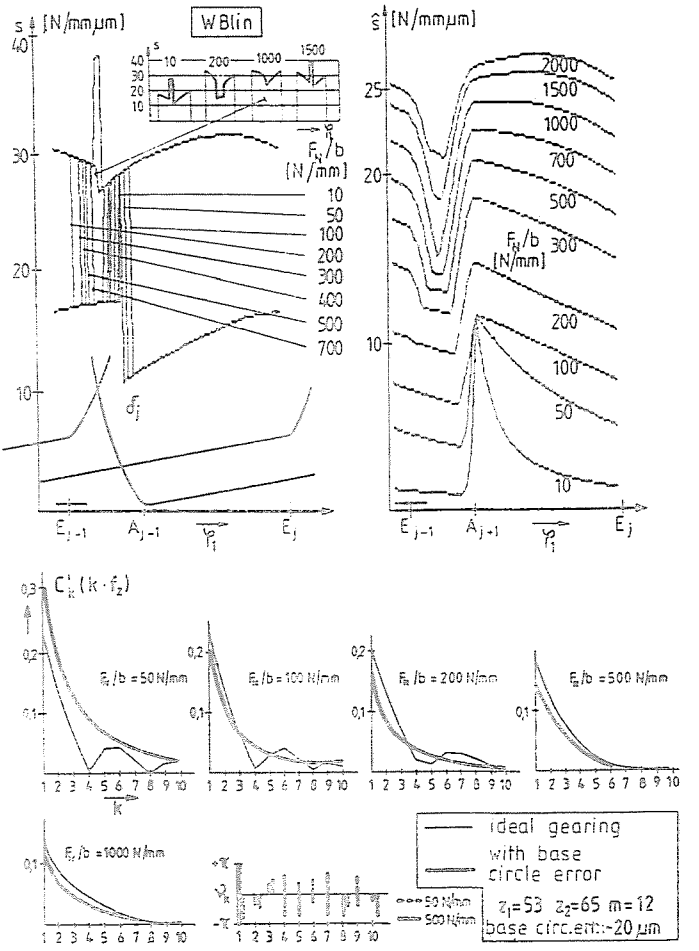

Fig. 13. Reduced stiffness and stiffness function for gear train with base circle error

The real resonance point locations do not correspond to the nominal ones, see *Fig. 14a*.

At higher load levels, the vibration extremities are decreased, but they are greater than for the ideal gear. Based on the simulation results, one can state that the greater vibration intensities, especially at lower specific load levels, result in increased dynamic loads, which is magnified by the decreased average damping, due to the real contact ratio decrease. Important nonlinear characteristics dominate the vibrations. At higher load levels the general vibration shape is similar to the ideal case, see *Fig. 14c* and *9b*, at low damping ratio. At normal damping, however, characteristic differences are found, see *Fig. 14d* and *Fig. 10c*.

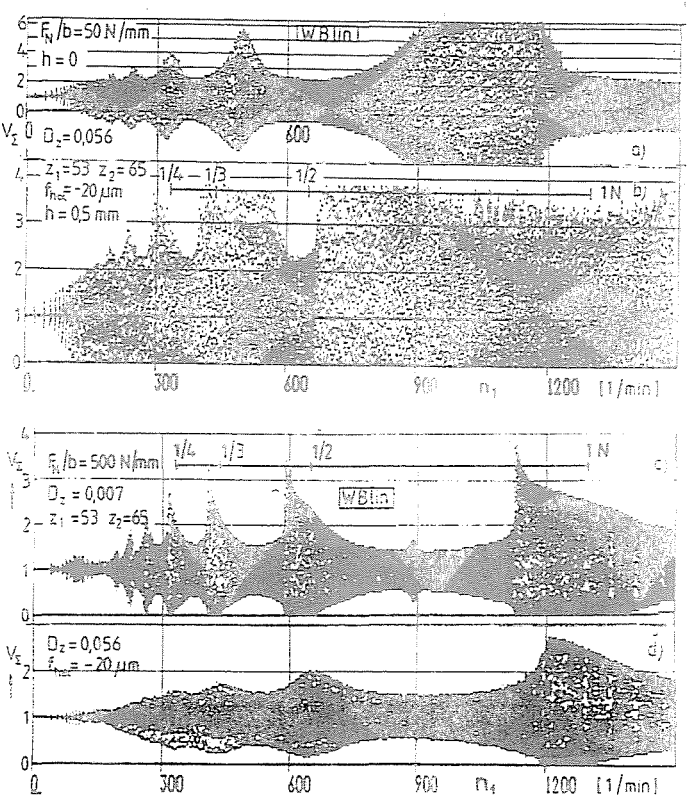

Fig. 14. Resonance curves for a gear train with base circle error

6. The Influence of the Pitch Error

For the study of the pitch error influence, $f_{pbr} = \pm 0.02$ mm error was taken on all drive gear teeth. For creating this type of error, it is enough to displace each second tooth profile: it results automatically an opposite sign pitch error with the following tooth flank. For the simulation, this gear was taken into meshing with a driven wheel of ideal tooth geometry, and WBlin type single tooth pair force-deflection characteristic was applied. The resulting reduced stiffness and the stiffness functions and the δ_j contact functions are presented on *Fig. 15*. The C'_k intensity components are represented on *Fig. 16*.

The basic period angle of the excitation and the stiffness function is now the double as previously. This corresponds to the fact that each second tooth is displaced with the given pitch error, giving so a double period. That is why new C'_k components appear, see *Fig. 16*. The k' values on *Fig. 16*

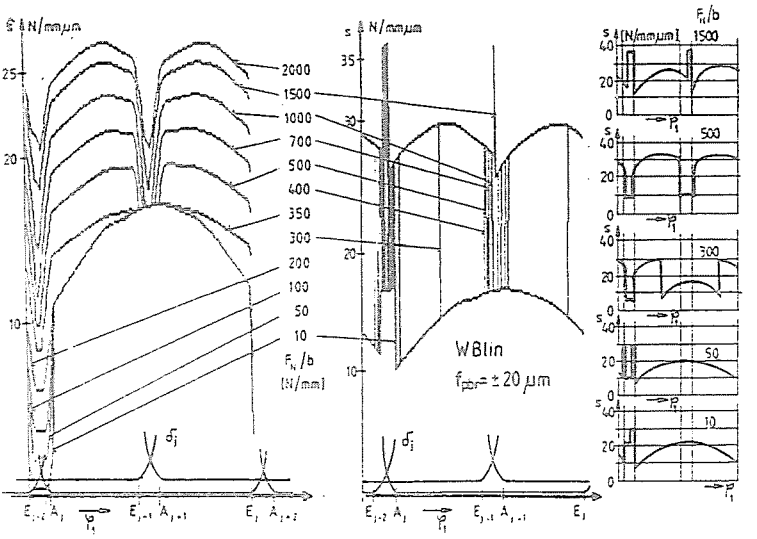

Fig. 15. Reduced stiffness and stiffness functions for a gear train with pitch error

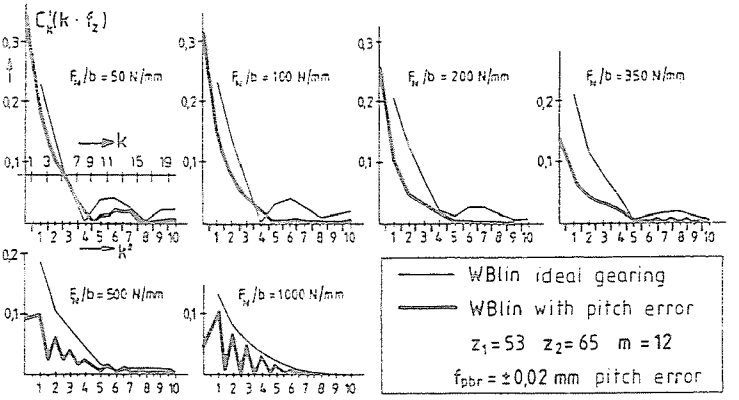

Fig. 16. Fourier components of the reduced stiffness function for gear with pitch error

refer to the Fourier indexes of the ideal tooth geometry. For the sake of comparison, the ideal gear component is indicated, too.

For the better presentation of the basic vibration characteristics, a simulation was realised with a low damping ratio, see *Fig. 17a*. In accordance with the new C'_k vibration excitation intensity factors, new resonance points appear; the resonance curve shape differs considerably from that for ideal gear

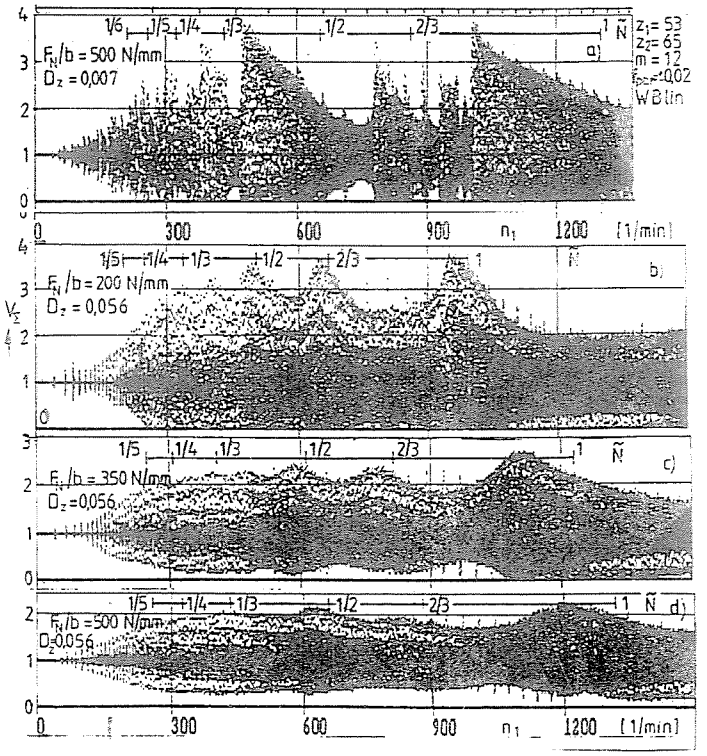

Fig. 17. Resonance curves for gear train with pitch error

geometry, see *Fig. 9a*. This characteristic remains even at higher damping ratios, see *Fig. 17bcd*. Above the input speed about n_1=200/min., the vibration peaks remain practically at the level of the resonance points. The maximum values at the main resonance point remain practically on the same level. So, intensive vibration is found on the whole speed region. An interesting result for that case that the resonances at $\tilde{N}$ =2/3 appear, which was not the case for normal gears.

The $\tilde{N}$ values on *Fig. 17* are similar to the previously defined N values, but they are calculated with the actual average stiffness, belonging to the given specific load.

7. Conclusions, Future Work

The simulation results of gear train dynamic analysis presented in this paper have shown ,that even in the case of ideal tooth geometry, important nonlinear effects develop. if the real tooth meshing conditions are taken into consideration. Similarly, the tooth errors involve important load dependent features. For enabling the treatment of these phenomena, a complex dynamic model is needed and careful tooth meshing analysis is to carry out. On the other side, the single tooth pair force-deflection curve type influences considerably the dynamic behaviour of the gear train, too.

Future work is needed for the study of the dynamic behaviour in the case of realistic gears with randomly distributed fabrication errors, and under continuously variable load conditions.

References

[1] MICHELBERGER, P. – ZOBORY, I.: Operation Loading Conditions of Ground Vehicles – Analysis of Load History. *Proceedings ASME Winter Annual Meeting*, Dallas, New York, 1990, pp. 175-182.
[2] ZOBORY, I.: The Forecasting of the Load Histories in the Drive Systems of Railway Traction Vehicles by Stochastic Simulation, Based on a System Dynamic Model. TU. Budapest, Dep. of Railway Vehicles. Research Report. 1992.
[3] NIEMANN, G. – WINTER, H.: Machine Elements. Bd. II. Springer Vlg. Berlin. Heidelberg, New-York. 1985. (In German.)
[4] MÁRIALIGETI, J.: Simulation Model of Gear Tooth Stiffness Function with Manufacturing Errors. *Periodica Polytechnica Ser. Transp. Eng.* Vol. 18. Nos 1-2. (1990) pp. 157–173.
[5] WINTER, H. – PODLESNIK, B.: Tooth Stiffness Characteristics of Gears. Part 2. *Antriebstechnik*, Vol. 22. (1983) Nr. 5. pp. 51–57.
[6] KLOTTER, K.: Vibration Theory. Bd. 1. Springer Vlg. Berlin, Heidelberg, New-York. 1980. (In German.)
[7] MÁRIALIGETI, J.: C. Sc. Thesis. Budapest, 1990. (In Hungarian.)
[8] Calculation of the Load Capacity of Gears. DIN 3990. (In German.)
[9] Tolerances for Gears. DIN 3961. 3962. 3963. (In German.)